Observations on Ground Motions of the 23 October 2011,Mw=7.2 Van, Turkey Earthquake

E. Harmandar & M. Erdik
Bogazici University, Kandilli Observatory and Earthquake Research Institute, Turkey

SUMMARY:
The Mw7.2 Van earthquake October 23rd, 2011 is estimated to have caused around 600 life losses and around 1 billion USD damage mainly due to total collapse of about 200 residential buildings and other lesser damaged buildings. The earthquake released its energy by thrust motion on an SW-NE trending blind fault. Different hypocenters from various agencies are reported. The Kandilli Observatory and Earthquake Research Institute (KOERI) hypocenter appears to correlate best to the damage seen. Shake-maps and ground motion estimates have been published by shows that the EMS intensities are estimated as above VIII within an area with 25 km diameter and that in the epicentral area the PGA values could have reached values of 0.5g. The Strong Motion Data Base of Turkey provides data from 22 stations most of them at large distances beyond 100 km. The closest stations are: Muradiye (Epicentral Distance = 49km, PGA=0.18g), Malazgirt (95km, PGA=0.06g), Bitlis Merkez (113km, PGA=0.1g) and Agri Merkez (123km, PGA=0.02g). The KOERI model is compatible with records of the Strong Motion Data Base of Turkey between 50 km and 120 km. We have complemented this strong motion data base through conversion of 20 broad-band seismographic data (in Turkey and Armenia) to acceleration and the 6 station accelerometric data obtained from Iran. We have also augmented the finite-fault simulation in the epicentral area through physical simulation of strong ground motion. A comparison of the prediction equation of strong ground motion is also included in the study.

Keywords: The October 23, 2011 Van earthquake, stochastic simulation, p-wave

1. INTODUCTION

On 23 October 2011 at 10:41 GMT, a major earthquake has struck Tabanlı, Van, located in Eastern Turkey with a magnitude of 7.2 (KOERI). About 120 aftershocks in magnitude ranges of 4.0 to 6.0 have been recorded within one week. Many people were affected by this quake and about 600 were dead. The earthquake caused major damage also to Van city center and Erciş province. Most buildings were significantly damaged or destroyed. According to the report provided by Prime Ministry Disaster and Emergency Management Presidency (AFAD, www.afad.gov.tr), 17.005 houses was identified as severe damage by December 9, 2011. Liquefaction and related ground deformations were evident and wide spread sand boils were observed particularly in Erciş Plain and the flood plain of Karasu River at the north of Van city. Also, there were a number of slope and embankment failures, and some of them reached to the Van-Ağrı Highway (Ulusay et al., 2012).

Although the total duration of the rupture was about 50 seconds, the major energy release occurred within 20 seconds (Konagai et al., 2012). The energy amount get out as result of earthquake is also major. The energy of main aftershock occurred on October 23, 2011 is 6.2 x 10^19 Nm (Yuji Yagi, 2012).

This study outlines the characteristics of the October 23, 2011 Van earthquake. The beta version (Böse, 2006) of stochastic finite-fault technique developed by Beresnev and Atkinson (1997, 1998) is used to model the ground motion from the October 23, 2011 Van Earthquake (Mw=7.2). The slip

model proposed by Yuyi Yagi (2012) is used to simulate the waveforms of data from Malazgirt and Muradiye stations. The results are discussed in terms of acceleration, Fourier Amplitude Spectrum. The observed data are also compared with the prediction equations.

2. GENERAL FEATURES OF THE VAN EARTHQUAKE

The most well-known seismic activity is probably induced by the North Anatolian Fault, a major strike-slip fault with a long history of damaging earthquakes. Another strike slip fault, the Eastern Anatolian Fault, lies around southwest from eastern Turkey to the Mediterranean with well-known large earthquakes. The Van earthquake took place with a failure on the southern boundary of the complex zone of continental collision between the Arabian Plate and the Eurasian Plate. These two regions have very different tectonics. To the east, in Iran, there is a great deal of convergence and mountain building as the Arabian plate to the south moves northwards into the Eurasian plate, as part of a belt of mountain building that runs all the way from the Alps to the Himalayas. To the west is the strike-slip faulting concentrated on the North and East Anatolian Faults, which is in response to the exact same continental collision (Rowan, 2012). The Lake Van basin is located between the Karlıova Joint and Zagros fault zone, north of the Bitlis suture belt (Selcuk et al., 2010) (Figure 2.1). The focal mechanism shows that the rupture was due to movement on an oblique thrust faulting (Figure 2.2), consistent with the expected tectonics in this region and aftershock activity. The geology and types of several faults in the region is very complicated.

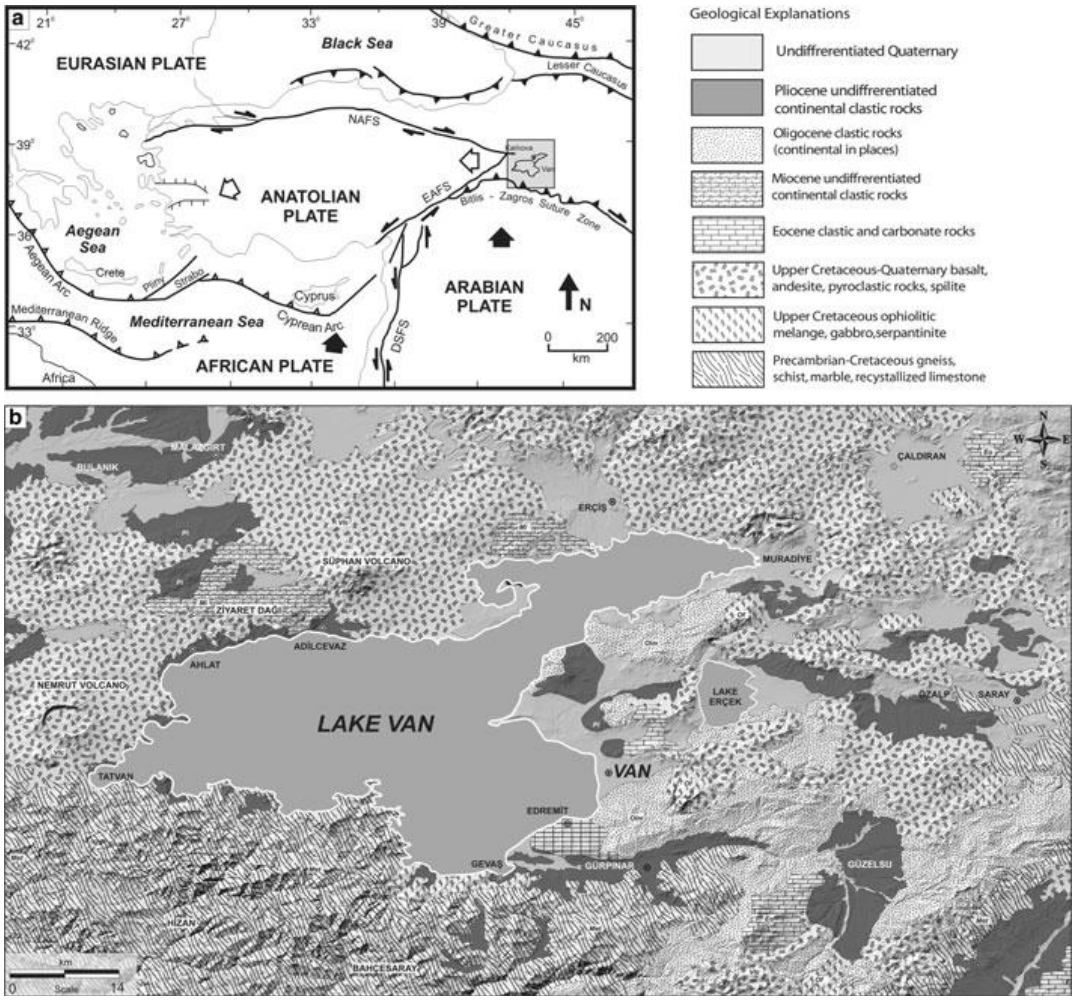

Figure 2.1. Representation of the faults and geology of Van region (Şengör et al., 1985)

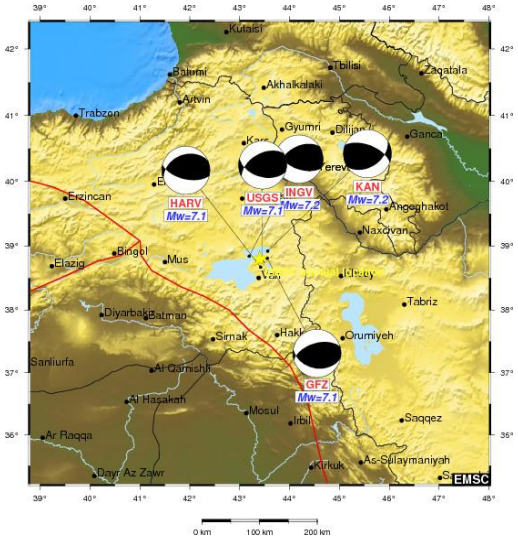

Figure 2.2. Source mechanism provided by different references (EMSC)

Lake Van basin consists of the metamorphic rocks of the Bitlis mountain ridge to the south of the lake; Pliocene-Quaternary deposits, carbonates and sandstones to the east, and volcanic deposits to the north and west, and the semi-active volcanoes Nemrut volcano and Süphan volcano in the vicinity of the lake (Schweizer, 1975; Lemcke, 1996). Van city and the towns of Gevaş, Gürpınar, Özalp, Muradiye, Çaldıran and Erciş are located over these young sediments (Selcuk et al., 2010).

The stress changes in the region due to this earthquake have interacted with other faults in the area. In this context, Van earthquake is associated with intense aftershock activity compared to the similar magnitude strike-slip earthquakes that took place in Turkey. Figure 2.3 shows the activity during October and November. The distribution of aftershocks with respect to time is also shown in Figure 2.3. The reason of intense aftershock activity is that the affected region has tectonically complex structure and there are several smaller faults with different properties.

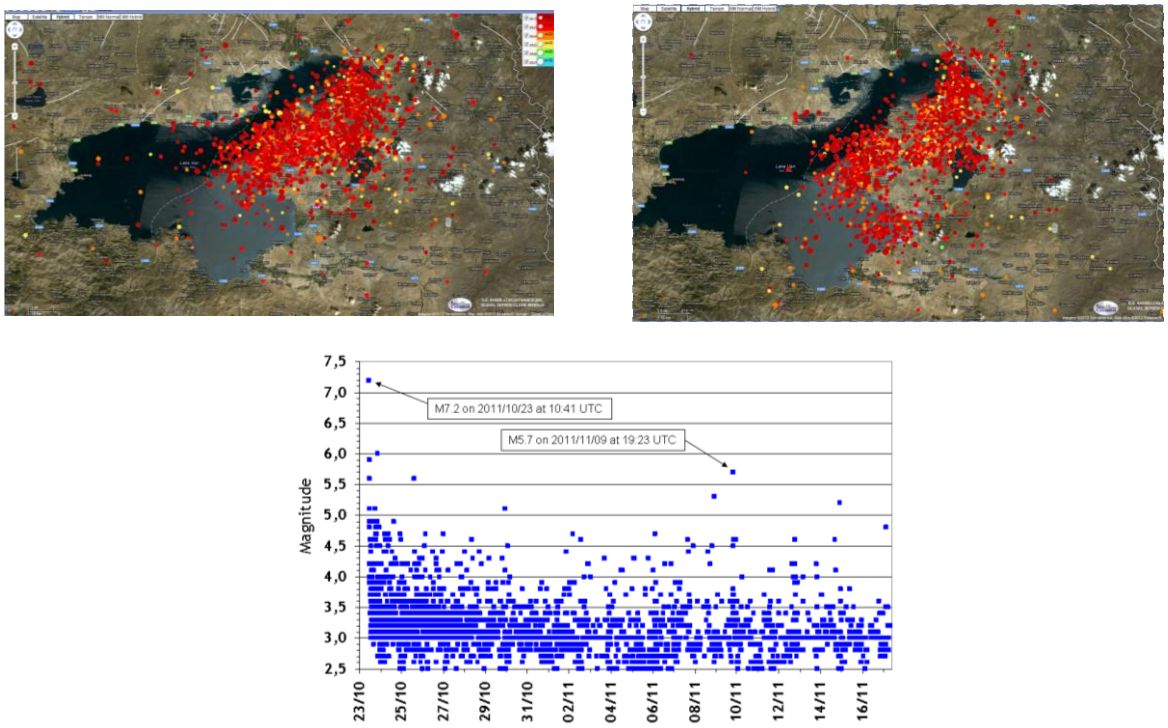

Figure 2.3. Aftershock activity on October (left) and November (right) and time distribution of the aftershocks (EMSC) (bottom)

3. DATA: RECORDED GROUND MOTIONS

The Van earthquake was recorded by 22 strong ground motion stations of the National Seismological Observation Network, operated by Prime Ministry Disaster and Emergency Management Presidency (AFAD) within 600 km of epicentre. Muradiye station with an epicentral distance of 42 km has an acceleration of 0.18g. The peak acceleration values of Malazgirt station within 95 km and Bitlis station within 116 km is 0.06 g and 0.104 g, respectively.

The earthquake was also recorded by 11 sets of digital accelerograph of Iran Strong Ground Motion Network (ISMN) (Figure 3.1). The maximum peak ground acceleration was recorded by Siah-Cheshmeh station (72 cm/s^2).

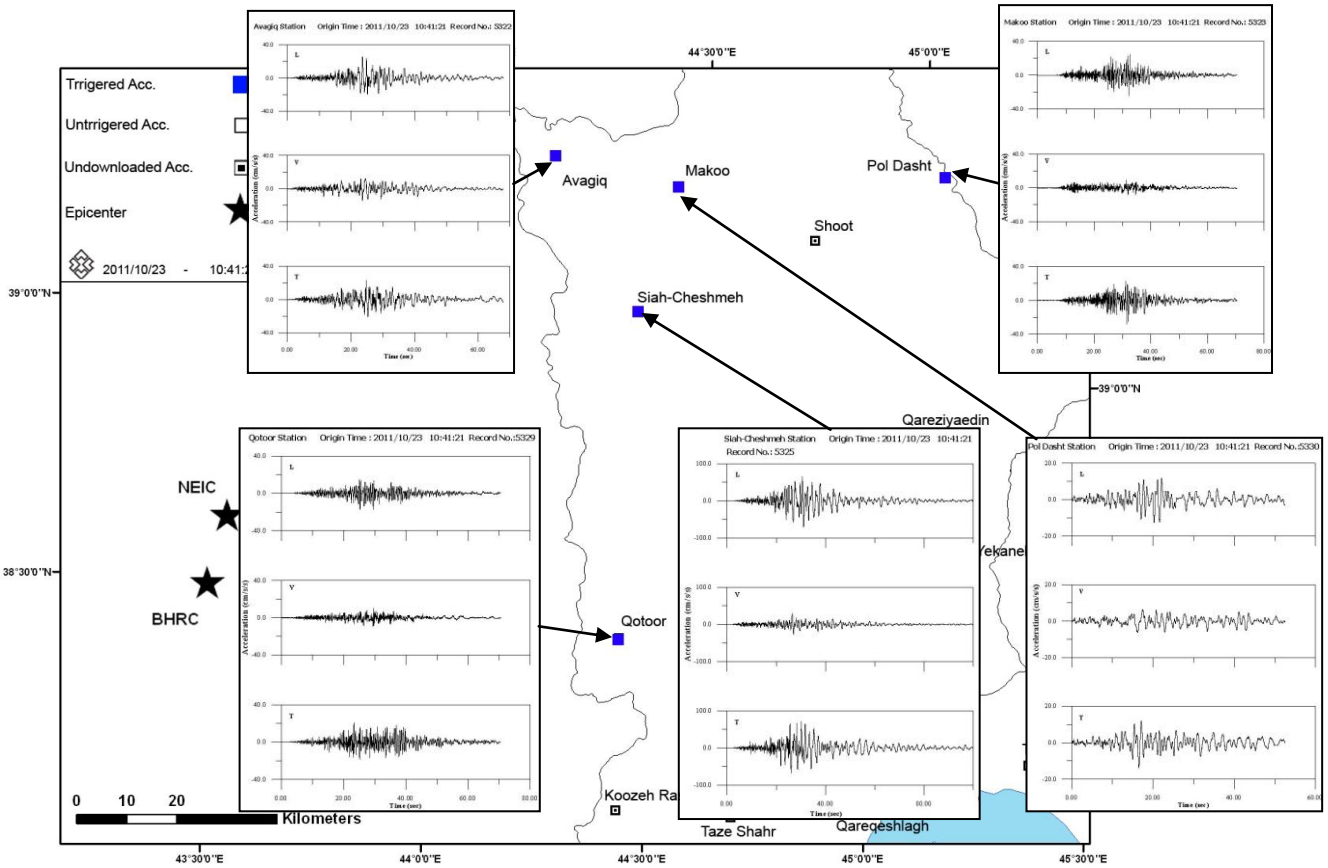

Figure 3.1. Strong ground motion data recorded by Iran Strong Ground Motion Network (http://www.bhrc.ac.ir/portal/Default.aspx?tabid=1106)

Additionally, seismometers, Geghard, Arzakan, Byurakan, in Armenia were recorded within epicentral distances around 200 km. Also, some seismometers operated by National Earthquake Monitoring Center (NEMC) in Kandilli Observatory and Earthquake Research Institute (KOERI) triggered during October, 23, 2011 Van earthquake (Figure 3.2). These seismometer data will lead to handle the long period issue.

4. METHOD: STOCHASTIC FINITE FAULT MODEL

The simulated ground motion in this study are obtained by using FINSIM (FINite fault SIMulation program) that based on the stochastic method for simulation of ground motion by Boore (1983), a commonly used technique assuming the earthquake as a point source. Boore's stochastic method is a simple but effective technique for predicting mean horizontal ground motions from shear waves by

considering the earthquake as a point source. It combines functional descriptions of the ground motion's amplitude spectrum with a random phase spectrum (Boore, 2003).

In FINSIM, Beresnev and Atkinson (1997, 1998) extended Boore's stochastic method by transferring it to finite faults. The fault plane is subdivided into smaller, rectangular subfaults of equal size representing separate point sources. Each subfault is treated as a point source, and each subevent has a ω-squared spectrum which is multiplied by the normalized spectrum of a limited-duration Gaussian noise sample in order to produce a subfault spectrum that has a stochastic character (Beresnev and Atkinson, 1997). A simple kinematic model of the Hartzell (1978) type is used to simulate the rupture propagation. The rupture starts at the hypocenter and propagates radially from it, triggering each subfault when the rupture front reaches its center. The subfault acceleration time history is propagated to the observation point through empirical distance-dependent duration, geometric attenuation and attenuation (Q) models. The ground motion at an observation point is obtained by adding up the contributions over all subfaults.

The FINSIM code by Beresnev and Atkinson (1997) was modified by Böse (2006). The modification had been done in two aspects: First, a correct time axis is required because we are interested in time differences between wave onsets at different seismic stations. Second, the stimulation and propagation of compressional waves have to be considered; compressional waves are less destructive than shear and surface waves but spread with higher velocities and are therewith the firstly recorded seismic waves at the sensor sites (Böse, 2006).

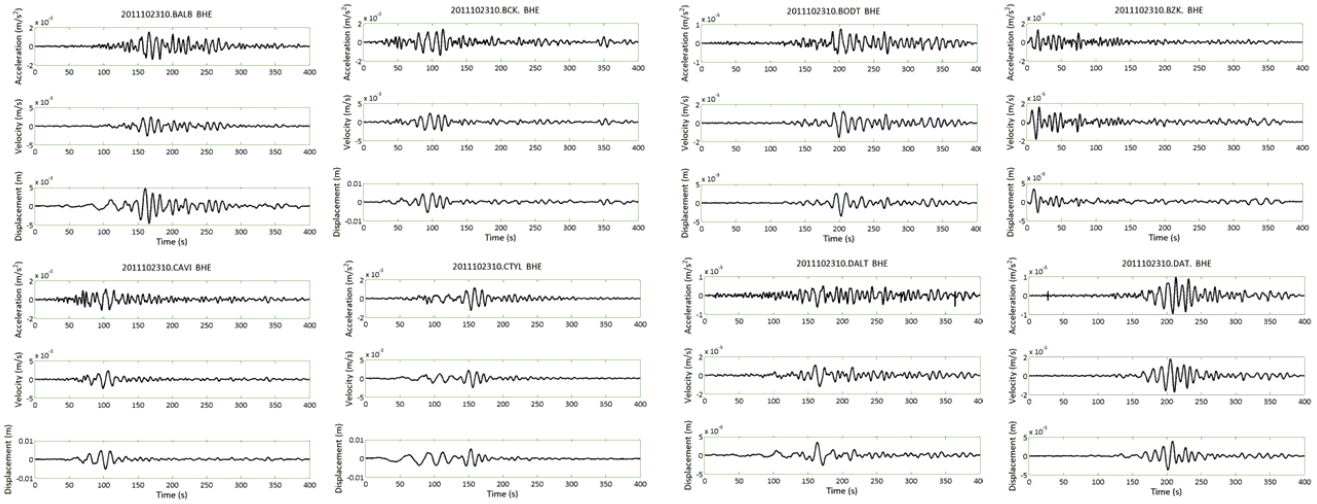

Figure 3.2. Some of weak motion data recorded by National Earthquake Monitoring Center (NEMC) in Kandilli Observatory and Earthquake Research Institute

5. MODELING PARAMETERS

In FINSIM, modeling of the finite source requires the orientation and dimensions of the fault plane, the dimensions of subfaults. The fault size is one of the most important parameter. Beresnev and Atkinson (1998) proposed a relation between the subfault size and magnitude:

$$\log \Delta L = -2.08 + 0.416M \quad (4 \le M \le 8) \tag{5.1}$$

where is the subfault size. We divide the fault plane (35/25 km) to 4x5 subfaults, and the fault plane (60/25 km) to 6x5 subfaults. The subfault corner frequency (fc) is calculated from

$$f_c = y\, z\, \beta / \pi \Delta L \tag{5.2}$$

where β is the shear wave velocity, y is the ratio of rupture velocity to shear wave velocity, set to as 0.9 (Rupture velocity is 3 km/sec), z is the product of strength factor, and taken as 1.68 for a standard rupture. Subfault rise time is expressed as

$$T = \Delta L / 2\, y\, \beta \tag{5.3}$$

Subfault moment (m0) is calculated by

$$m_0 = \Delta\sigma\, \Delta L^3 \tag{5.4}$$

where is the stress parameter and controls each subfault moment and as well as total moment. The stress parameter is set to a value of 40 bars to avoid an inadequate number of active subsources (Beresnev, 1997).

In the simulation procedure, the number of subfaults added is constrained by the conservation of seismic moment. To achieve the target moment, the elementary faults are allowed to triggered ns times, calculated as

$$n_s = M_l / l\, m\, M_e \tag{5.5}$$

where Ml is the target-fault and Me is the subfault moments; l and m are the number of elements along the length and width of fault; ns is the nearest integer of the ratio. Geometrical spreading, anelastic and near-surface attenuations are the parameters controlling the effects of the propagation path. Several models are tried for the path effects. Any empirical analysis to assume the parameters related to the path effects have not been done due to the lack of observed data. For the geometric attenuation model, 1/R model, which makes the residuals between the observed and simulated data less, is used.

The source model used in analyses is represented in Figure 5.1. The rupture process is estimated by using a new earthquake source inversion (Yagi & Fukahata, 2011) of teleseismic body waves (P-waves) data recorded at GSN provided by IRIS-DMC.

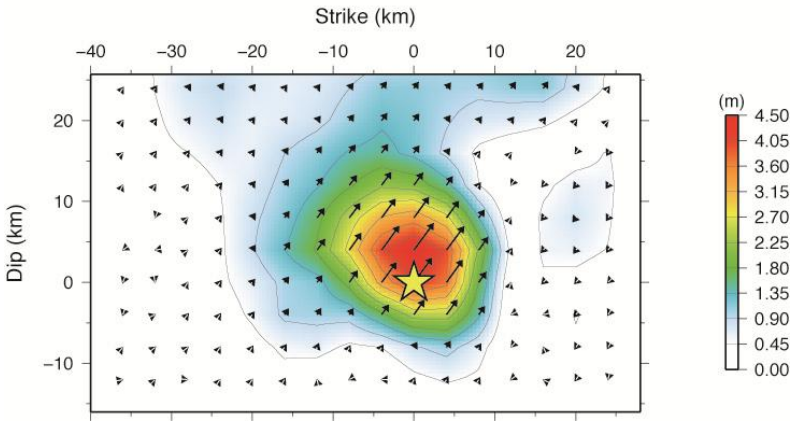

Figure 5.1. Slip distribution proposed by Yagi, 2012 (http://www.geol.tsukuba.ac.jp/~yagi-y/EQ/2011_E_Turkey/index_e.html)

The source location determined by KOERI is used. The source dimensions are defined as 50 km x 35 km based on Yuyi Yagi model. Strike and dip angles are chosen as 239° and 51° (Yagi, 2011). The fault plane is divided into 10 x 7 subfaults, assigning a subfault dimension of 5 km x 5 km. Hermann (1985) model is used for the crustal shear-wave quality factor. The source parameters are listed in Table 5.1.

Table 5.1. Modeling parameters

Parameter	Parameter value
Fault orientation	Strike 239^o, dip 51^o
Fault dimensions along strike and dip (km)	50 by 35
Stress parameter (bars)	100
Subfault dimensions (km)	5 by 5
Distance-dependent duration term (sec)	T_o+0.01R
Inelastic attenuation $Q(f)$	$88f^{0.9}$
Windowing function	Saragoni-Hart
Kapa	0.05 (NEHRP soil site)
Crustal-shear wave velocity (km/sec)	3.3
Crustal density (g/cm^3)	2.7

6. RESULTS AND DISCUSSION

Results of finite-fault simulations are compared against the recorded accelerations and their corresponding Fourier amplitude spectra. Acceleration waveforms are generated for the closest stations, Muradiye and Malazgirt, to the epicentre of Van earthquake. Figure 6.1 shows the horizontal components of the recorded accelerograms of Muradiye station and their corresponding simulated time series.

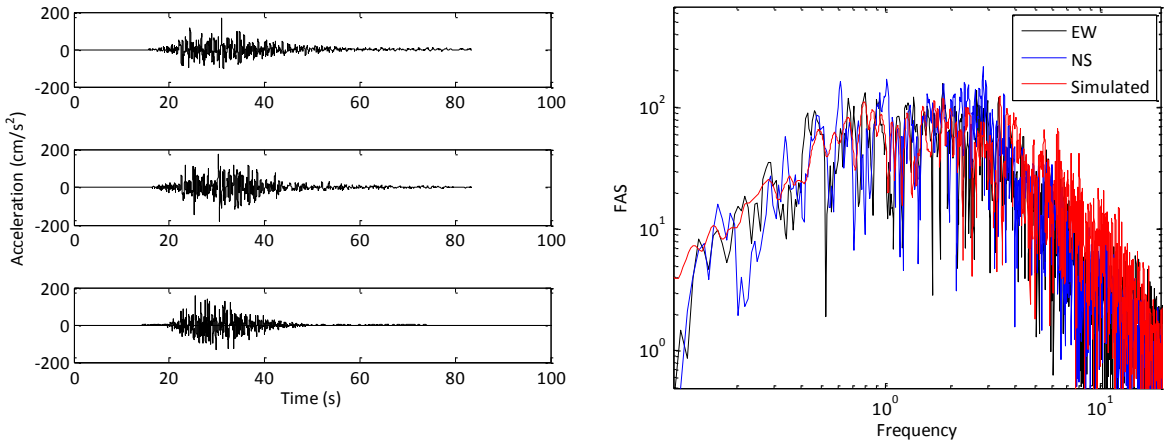

Figure 6.1. Recorded (first two rows) and simulated accelerograms (bottom row) with their corresponding Fourier amplitude spectra (Muradiye station within an epicentral distance of 42 km)

We observe that the individual synthetic PGA values generally match well with the observations. The duration of the ground motions is well reproduced. Figure 6.1 also shows the Fourier spectra of the simulated record together with the observed spectra. The observed and simulated spectra show a good agreement within the intermediate frequency ranges (1-5 Hz). At high frequencies, the simulated amplitude spectrum overestimates the observed spectra. This can be explained by the stress drop or crustal shear-wave quality factor.

Figure 6.2 compares the synthetic acceleration time histories and Fourier amplitude spectra to those of recorded horizontal components at Malazgirt station.

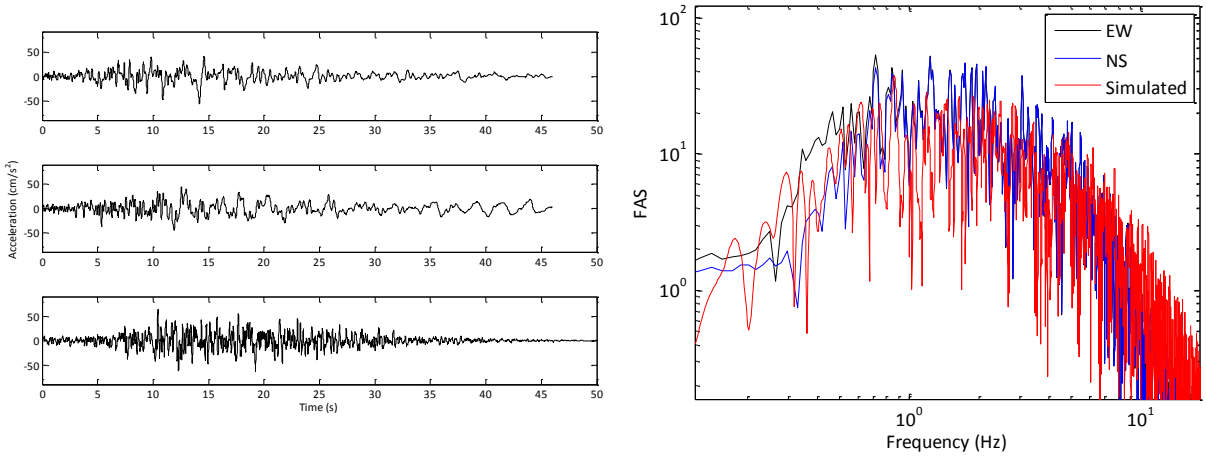

Figure 6.2. Recorded (first two rows) and simulated accelerograms (bottom row) with their corresponding Fourier amplitude spectra (Malazgirt station within an epicentral distance of 95 km)

For the Malazgirt case, the consistency of observed and simulated PGA values is not as successful as the Muradiye case. On the contrary to Muradiye, simulated Fourier spectrum is in good agreement with simulated spectra for low and high frequencies. However, simulated Fourier amplitude spectrum underestimates the observed at the intermediate frequency range. This misfit can be due the source model or homogeneous half-space assumption of the model.

The validation of source parameters will be more reliable as best-fit of observed and simulated data for other stations is provided.

Additionally, strong ground motion data are compared with the ground motion prediction equations (Figure 6.3).

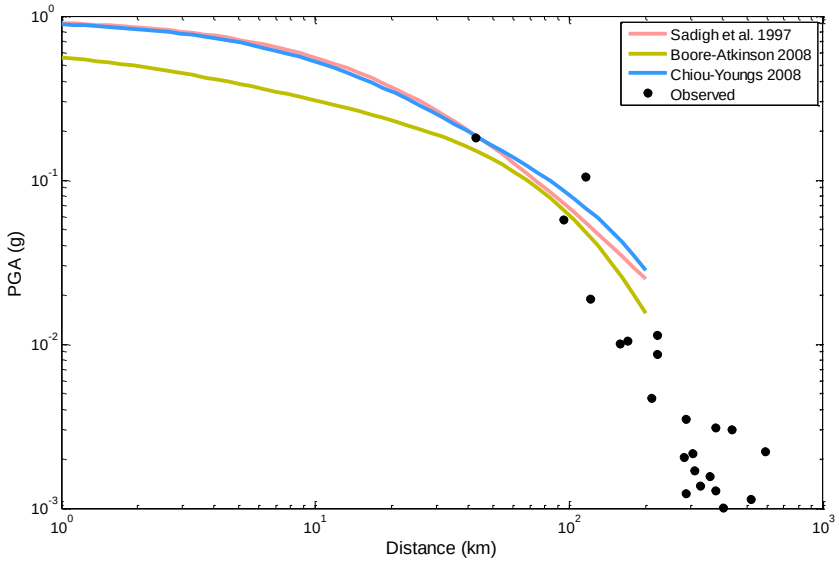

Figure 6.3. Comparison of attenuation of observed data with ground motion prediction equations

7. CONCLUSIONS

The October 23, 2011 Van earthquake (M_W=7.2) was felt over a large area in the eastern and southeastern parts of Turkey. The earthquake caused about 640 fatalities and very heavy damage to buildings in the province of Erciş, Van city centre and villages. The fault mechanism of earthquake is east-west oriented thrust fault mechanism. The Van earthquake was associated with fault that was not

previously recognized as active. Intense aftershock activity has been occurred after the main-shock. 16 temprory seismic instruments were deployed by KOERI to observe the activity in the region after the main shock. Another earthquake (Van-Edremit earthquake) took place at 10 km to the south of Van city, near Edremit province during the very intense aftershock activity. Six accelographs were triggered by this earthquake. There was high damage in the City of Van as compared to the light damage in Edremit.

The Van earthquake caused greater damage in Erciş compared to Van city centre. The reason is appeared to be that Erciş City is located on hanging wall part of the thrust rupture that may imply higher levels of ground motion than Van City. Directivity effect can be clearly observed in particle motions.

In this study, stochastic simulation of the region also has studied. The results of simulation are preliminary in the sense that so far two stations have been studied. It is expected that the source parameters will stabilize with comparing more observed and simulated data and the spatial distribution of ground motion parameters become more reliable. We also note that after the validation of source parameters distribution of peak ground-motion parameters will be studied and compared with the building damage distribution in the near-fault region most affected by the seismic shaking

AKCNOWLEDGEMENT

We thank Maren Böse for providing the computer program FINSIM-beta. We thank Prof. Ali Pınar for his advice on source model.

REFERENCES

Beresnev, I.A., Atkinson, G.M. (1997). Modeling finite-fault radiation from the ωn spectrum. Bull. Seismol. Soc. Am. 87, 67-84.

Beresnev, I.A., Atkinson, G.M. (1998). FINSIM - a FORTRAN program for simulating stochastic acceleration time histories from finite faults. *Seism. Res. Lett*. **69**, 27-32.

Boore, D.M. (1983). Stochastic simulation of high frequency ground motions based on seismological models of radiated spectra. *Bull. Seismol. Soc. Am*. **73**, 1865–1894.

Boore, D.M. (2003). Simulation of ground motion using the stochastic method. *Pure Appl. Geophys*. **160,** 635-676.

Boore, D. and Atkinson, G. (2008). Ground-motion prediction equations for the average horizontal component of PGA, PGV, and 5%-damped SA at spectral periods between 0.01s and 10.0 s. *Earthquake Spectra*, **24**, 99-138.

Böse M. (2006). Earthquake Early Warning for Istanbul using Artificial Neural Networks, Ph.D. thesis, Universität Karlsruhe (TH).

Chiou, B. S.-J., and Youngs, R. R., (2008). An NGA model for the average horizontal component of peak ground motion and response spectra, *Earthquake Spectra*, **24**, 173-216.

Hartzell, S.H. (1978). Earthquake aftershocks as Green's functions. *Geophys. Res. Lett*. **5**, 1-4.

Herrmann, R. B. (1985). An extension of random vibration theory estimates of strong ground motion to large earthquakes. *Bull. Seismol. Soc. Am*. **75**, 1447–1453.

Konagai, K., Ulusay, R., Kumsar, H., Aydan, Ö. and Çelebi, M.. (2012). The characteristics of seismic, strong motion and structural damage of the 2011 Van-Erciş earthquake. *Proc. Int. Symp. Eng. Lessons Learned from the great East Japan Earthquake,* March 1-4, Tokyo, Japan.

Lemcke, G. (1996). Pala oklimarekonstruktion am Van See (Ostanatolien, Turkei). Dissertation, Swiss Federal Institute of Technology (Zurich) 11786:182.

Rowan, C. (2012). http://blogs.scientificamerican.com/guest-blog/2011/10/27/a-geologist-eye-view-of-the-van-earthquake/.

Sadigh, K., Chang, C. -Y. , Egan, J. A., Makdisi, F. and Youngs, R. R. (1997). Attenuation relationships for shallow crustal earthquakes based on California strong motion data. *Seismological Research Letters*, **68(**1), 180-189.

Schweizer, G. (1975). Untersuchungen zur Physiogeographievon Ostanatolienund Nordwestiran. Geomorphologische, klima- und hydrogeographischeStudien im Vansee- und Rezaiyehsee-Gebiet. Tubinger Geographische Studien 60.

Selcuk, L., Selcuk, A. S. and Beyaz, T. (2010). Probabilistic seismic hazard assessment for Lake Van basin, Turkey. *Nat. Hazards*. **54**, 949-965.

Şengör, A. M. C., Görür, N. and Şaroğlu, F. (1985). Strike-slip faulting and related basin formation in zones of tectonic escape: Turkey as a case study, Strike-slip Deformation, Basin Formation, and Sedimentation. *Soc. Econ. Paleont. Min. Spec. Pub. 37 (in honor of J.C. Crowell)*, 227-264.

Ulusay, R., Kumsar, H., Konagai, K. and Aydan, Ö. (2012). The characteristics of geotechnical damage by the 2011 Van-Erciş earthquake. *Proc. Int. Symp. Eng. Lessons Learned from the great East Japan Earthquake,* March 1-4, Tokyo, Japan.

Yagi, Y. and Fukahata, Y. (2011). Introduction of uncertainty of Green's function into waveform inversion for seismic source processes. *Geophys. J. Int*. **186**, 711-720.

Yagi, Y., (2012). (http://www.geol.tsukuba.ac.jp/~yagi-y/EQ/2011_E_Turkey/index_e.html)